

# Molecular Dynamics of DNA Quadruplex Molecules Containing Inosine, 6-Thioguanine and 6-Thiopurine

Richard Štefl,<sup>\*†</sup> Nad'a Špačková,<sup>‡§||</sup> Imre Berger,<sup>\*\*</sup> Jaroslav Koča,<sup>\*</sup> and Jiří Šponer<sup>†§</sup>

<sup>\*</sup>Laboratory of Biomolecular Structure and Dynamics, <sup>†</sup>Department of Theoretical and Physical Chemistry, and <sup>||</sup>Department of Physical Electronics, Faculty of Science, Masaryk University, 611 37 Brno, Czech Republic; <sup>‡</sup>Institute of Biophysics, Academy of Sciences of the Czech Republic, 612 65 Brno, Czech Republic; <sup>§</sup>J. Heyrovský Institute of Physical Chemistry, Academy of Sciences of the Czech Republic, 182 23 Prague, Czech Republic; and <sup>\*\*</sup>Institute for Molecular Biology and Biophysics, CH-8093 Zürich, Switzerland

**ABSTRACT** The ability of the four-stranded guanine (G)-DNA motif to incorporate nonstandard guanine analogue bases 6-oxopurine (inosine, I), 6-thioguanine (tG), and 6-thiopurine (tl) has been investigated using large-scale molecular dynamics simulations. The simulations suggest that a G-DNA stem can incorporate inosines without any marked effect on its structure and dynamics. The all-inosine quadruplex stem d(III)<sub>4</sub> shows identical dynamical properties as d(GGG)<sub>4</sub> on the nanosecond time scale, with both molecular assemblies being stabilized by monovalent cations residing in the channel of the stem. However, simulations carried out in the absence of these cations show dramatic differences in the behavior of d(GGG)<sub>4</sub> and d(III)<sub>4</sub>. Whereas vacant d(GGG)<sub>4</sub> shows large fluctuations but does not disintegrate, vacant d(III)<sub>4</sub> is completely disrupted within the first nanosecond. This is a consequence of the lack of the H-bonds involving the N2 amino group that is not present in inosine. This indicates that formation of the inosine quadruplex could involve entirely different intermediate structures than formation of the guanosine quadruplex, and early association of cations in this process appears to be inevitable. In the simulations, the incorporation of 6-thioguanine and 6-thiopurine sharply destabilizes four-stranded G-DNA structures, in close agreement with experimental data. The main reason is the size of the thiogroup leading to considerable steric conflicts and expelling the cations out of the channel of the quadruplex stem. The G-DNA stem can accommodate a single thioguanine base with minor perturbations. Incorporation of a thioguanine quartet layer is associated with a large destabilization of the G-DNA stem whereas the all-thioguanine quadruplex immediately collapses.

## INTRODUCTION

The guanine (G) quadruplex motif is among the most interesting unusual conformations that DNA can adopt. DNA sequences with stretches of guanine residues that are capable of forming this four-stranded structure occur at the ends of eukaryotic chromosomes, the telomeres (Akman et al., 1991; Cech, 1988; Han et al., 1999b; Henderson et al., 1987; Klobutcher et al., 1981; Lipps et al., 1982; Marathias et al., 1999; Mergny et al., 1999; Moyzis et al., 1988; Murchie and Lilley, 1992; Oka and Thomas, 1987; Read et al., 1999; Sen and Gilbert, 1988; Sundquist, 1993; Sundquist and Heaphy, 1993; Sundquist and Klug, 1989; Williamson et al., 1989). The capability of telomeric DNA sequences to adopt this unusual DNA conformation renders them particularly attractive as a target in anti-cancer therapy (Mergny et al., 1999). Quadruplex molecules containing guanine bases have been well characterized by x-ray (Kang et al., 1992; Laughlan et al., 1994; Phillips et al., 1997) and NMR (Aboul-ela et al., 1994; Hud et al., 1999; Schultze et al., 1999; Smith and Feigon, 1992; Smith et al., 1995; Strahan et al., 1998) techniques and also studied in detail by large-scale molecular dynamics (MD) simulations (Špačková et al., 1999), providing interesting insight into the structural

and dynamical properties of the four-stranded G-DNA stem formed by consecutive guanine quartets. G-DNA is an exceptionally stable and rigid DNA form possessing unique mechanical properties (Špačková et al., 1999, submitted). Monovalent cations lining up in the channel of the G-DNA stem represent an integral part of these molecular assemblies. MD simulations showed that the G-DNA stem can sustain a reduction of the number of monovalent cations in the channel without any marked destabilization (Špačková et al., 1999). This allows a smooth exchange of the ions with the solvent. On the other hand, a G-DNA stem without any cation is unstable and can either disintegrate or undergo stabilization by spontaneous interception of cations from the solvent. The latter process is more likely and we recently estimated that a vacant G-DNA stem would spontaneously attract a cation on a scale of ca 10 ns (Špačková et al., submitted). Besides the all-guanine GGGG quartet, the four-stranded G-DNA stem can also incorporate other base quartet arrangements. Well-characterized G-DNA quadruplex structures containing such quartets are antiparallel G-DNA molecules with mixed guanine/cytosine GCGC quartets (Bouaziz et al., 1998; Kettani et al., 1995, 1998). Such quadruplexes have been studied by high-resolution NMR techniques (Bouaziz et al., 1998; Kettani et al., 1995, 1998) and MD simulations (Špačková et al., submitted).

Although the atomic resolution experiments and simulations provide a consistent picture of the final status of the G-DNA stem and the role of cations in its stabilization (Aboul-ela et al., 1994; Bouaziz et al., 1998; Hud et al., 1999; Kang et al., 1992; Kettani et al., 1995, 1998; Laugh-

Received for publication 3 May 2000 and in final form 28 September 2000.

Address reprint requests to Dr. Jiří Šponer, J. Heyrovský Institute of Physical Chemistry, Academy of Sciences of the Czech Republic, Dolejškova 3, 182 23 Prague, Czech Republic. Tel.: 420-2-6605-3776; Fax: 420-2-858-2307; E-mail: sponer@indy.jh-inst.cas.cz.

© 2001 by the Biophysical Society

0006-3495/01/01/455/14 \$2.00

lan et al., 1994; Phillips et al., 1997; Schultze et al., 1999; Smith and Feigon, 1992; Smith et al., 1995; Špačková et al., 1999, submitted; Strahan et al., 1998), much less is known about the processes leading to a formation of the G-DNA stem. Formation of a G-DNA assembly is a long process that takes hours to days. Experiments indirectly indicate that duplexes as well as other intermediate structures are involved in quadruplex formation (Han et al., 1999a; Hardin et al., 1997). MD simulations revealed that a G-DNA stem can adopt alternative cation-stabilized folds with shifted strands having structural properties closely resembling the native stem (Špačková et al., 1999). Such structures were suggested to be possible metastable states during the very last stages of the formation of the final G-DNA stem.

The four-stranded G-DNA stem should be entirely capable of incorporating the guanine analog 6-oxopurine (inosine, I). Inosine quartets lack hydrogen bonds involving the guanine amino group. Apart from that, however, they would exhibit exactly the same coordination of the ions as in the channel of the guanine quadruplex as the electronic structure and molecular electrostatic potential of inosine and guanine are similar (Šponer et al., 1996). Indeed, poly-rI is assumed to form the quadruplex structure (Arnott et al., 1974). Quadruplex molecules analogous to the guanine quadruplex could be formed also by 6-thioguanine or even 6-thiopurine, as the electronic structure of 6-thioguanine is similar to guanine with even a larger molecular dipole moment (Šponer et al., 1997, 1999). Molecular interactions of thioguanine have been extensively characterized by ab initio quantum chemical calculations (Šponer et al., 1997, 1999). Thioguanine has similar intrinsic H-bonding and stacking properties as guanine, although H-bonds involving thioguanine show a slightly reduced electrostatic contribution whereas the dispersion attraction is enhanced. On the other hand, the 6-thio-group is very poorly hydrated compared with the 6-oxo-group, and thus replacement of thioguanine by guanine was suggested to have a pronounced effect on the DNA hydration pattern (Šponer et al., 1997). The thio group shows also uniquely strong interactions with soft metals such as  $\text{Cd}^{\text{II}}$ ,  $\text{Hg}^{\text{II}}$ , and  $\text{Pt}^{\text{II}}$  (Šponer et al., 1999).

However, experiments clearly show that 6-thioguanine inhibits a formation of a quadruplex in the presence of  $\text{K}^+$  (Gee et al., 1995; Marathias et al., 1999; Olivas and Maher, 1995; Rao et al., 1995). The experiments do not explain whether the reason for this is found in the absolute instability of such an assembly or the existence of other more stable structures competing with the quadruplex. Also, the experiments do not reveal whether the destabilization of G-DNA by 6-thioguanine is primarily due to a weak interaction between the thio group and the cations, or due to steric reasons associated with the size of the thio group. 6-Thioguanine was also found to have an influence on the stability and structure of duplexes (Marathias et al., 1999) although there appear to be no substantial effects on triplex formation (Gee et al., 1995; Marathias et al., 1999; Olivas

and Maher, 1995; Rao et al., 1995). Inhibition of G-DNA formation via insertion of thioguanine is important because it facilitates triplex formation at a physiological concentration of  $\text{K}^+$  (Gee et al., 1995; Marathias et al., 1999; Olivas and Maher, 1995; Rao et al., 1995).

Various aspects of the structure and dynamics of quadruplex molecules have been addressed in computational studies (Hardin and Ross, 1994; Mohanty and Bansal, 1995, 1994; Špačková et al., 1999, submitted; Strahan et al., 1994). Recent qualitative advances in all-atom MD simulations (implementation of accurate methods for the long-range electrostatic interactions (Cheatham et al., 1995) and refinement of the DNA force fields (Cheatham et al., 1999; Cornell et al., 1995; Follope and MacKerrel, 2000; Langley, 1998) allowed unprecedented improvements in the molecular modeling of nucleic acids (Feig and Pettitt, 1998, 1999; Cheatham et al., 1998; Konerding et al., 1999; Louise-May et al., 1996; Shields et al., 1997; Sprous et al., 1999; Trantírek et al., 2000; Weerasinghe et al., 1995; Young and Beveridge, 1998; Young et al., 1997) including studies of four-stranded assemblies (Špačková et al., 1998, 1999, submitted). In the present study we use state-of-the-art MD techniques to carry out a set of unconstrained nanosecond-scale MD simulations of parallel quadruplex stems  $d(\text{NNNN})_4$  incorporating guanine (G), 6-oxoguanine (inosine, I), 6-thioguanine (tG), and 6-thiopurine (tI) ( $\text{N} = \text{G}, \text{I}, \text{tG}, \text{or tI}$ ) as well as mixed antiparallel structures  $d(\text{NCNN})_4$  (Figs. 1 and 2). We pursued two objectives by carrying out these simulations. First, we aimed at comparing the ability of G and I to form quartet structures and answer the ques-

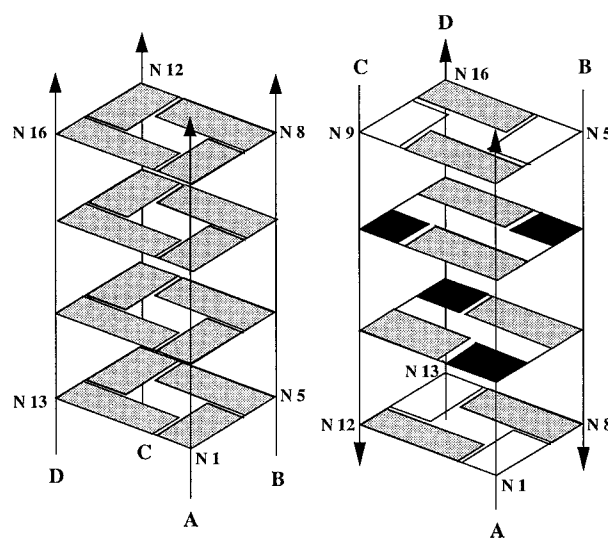


FIGURE 1 Quadruplex topologies and nucleobase quartets investigated in this paper. Molecular structure of the parallel  $d(\text{NNNN})_4$  stem is shown on the left and the antiparallel  $d(\text{NCNN})_4$  stem is shown on the right;  $\text{N} = \text{G}$  or  $\text{I}$ . Cytosine bases in anti conformation are in black, purine bases in syn conformation are in white, and purine bases in anti conformation are in gray.

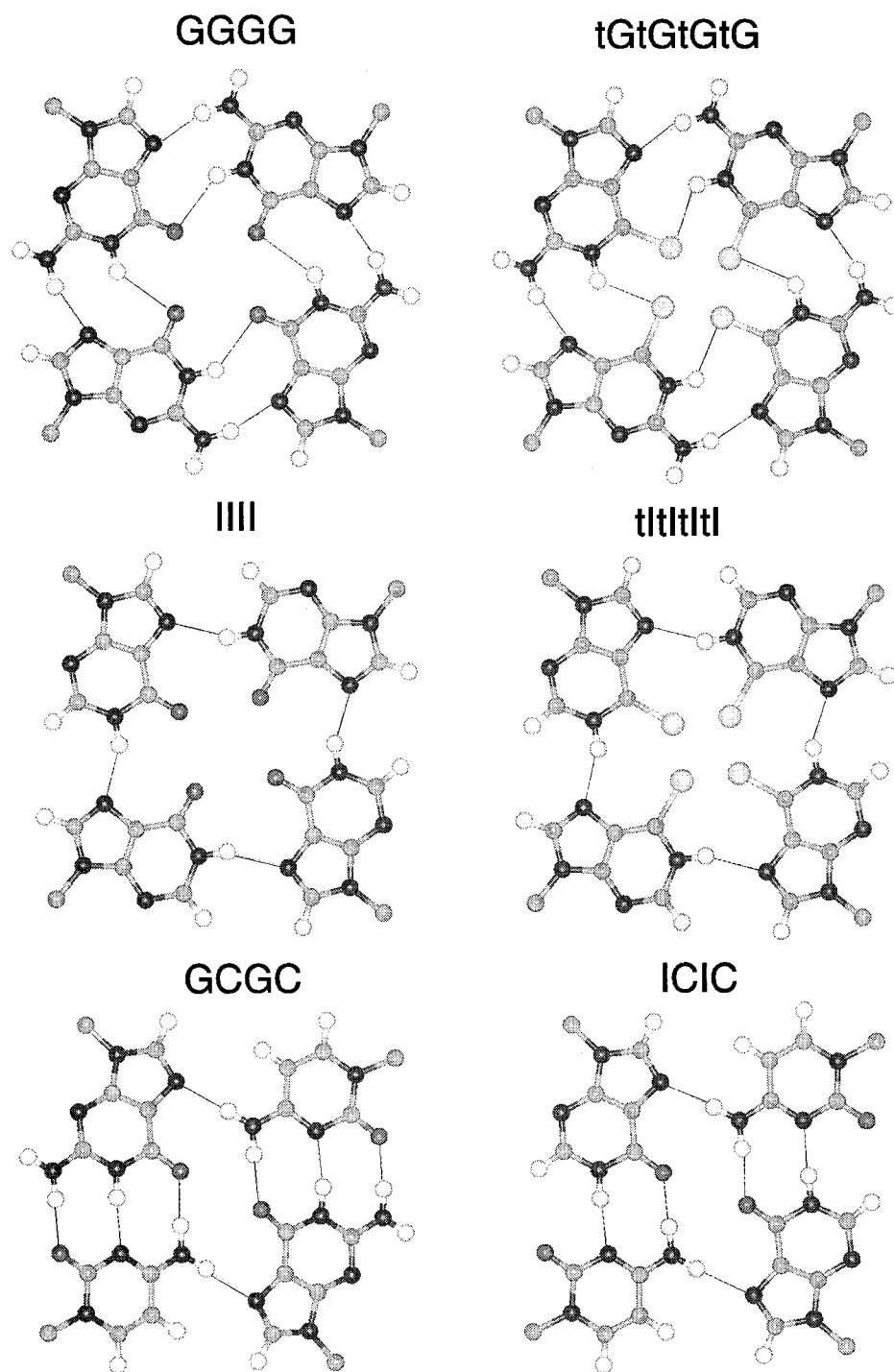


FIGURE 2 Nucleobase quartets investigated in this paper.

tion why thioguanine inhibits a formation of quadruplexes. Second, by simulating quadruplex stems with different compositions and different stabilities, we aimed to obtain more information about the general principles underlying the stabilization of these molecular assemblies and a further insight into their folding path. The simulations show that inosine can form stable quadruplex stems  $d(\text{III})_4$  and  $d(\text{IC})_4$  with all structural and dynamical properties essen-

tially identical to the native G-DNA stem on the nanosecond time scale. The simulations nevertheless indirectly show that  $d(\text{III})_4$  is less stable than  $d(\text{GGGG})_4$  due to the absence of one of the H-bonds. More importantly, we suggest that the lack of the guanine amino group causes certain structures that might be semi-stable intermediates in the formation of the  $d(\text{GGGG})_4$  quadruplex to be unstable in the case of  $d(\text{III})_4$ . Thus, we speculate that a formation of  $d(\text{III})_4$

can proceed via different intermediates than a formation of  $d(\text{GGGG})_4$ . It is also possible that the formation of  $d(\text{III})_4$  may be kinetically hindered compared to  $d(\text{GGGG})_4$ . The simulations show that the  $d(\text{tGtGtGtG})_4$  and  $d(\text{tTtTtTtT})_4$  parallel quadruplexes exhibit absolute instability on the nanosecond scale, the primary reasons being steric problems associated with the size of the thiogroup.

## METHODS

### Molecular dynamics simulations

All simulations were carried out using the AMBER 5.0 (Case et al., 1997; Pearlman et al., 1995) program with a Cornell et al. (1995) force field. The nucleic acid molecules were surrounded by a periodic box of water molecules described by the TIP3P potential (Jorgensen et al., 1983). The periodic box was extended to a distance of 10 Å from any solute atom. The number of explicit water molecules included in the simulations was ~2700. The molecules were neutralized by  $\text{Na}^+$  cations using standard parameters for the Cornell et al. force field (Cornell et al., 1995; Hardin and Ross, 1994). Missing parameters for 6-oxopurine, 6-thioguanine, and 6-thiopurine were obtained in the following way. The ESP charges have been derived using the Hartree-Fock approximation with the 6-31G\* basis set of atomic orbitals, consistent with the other parts of the force field. The missing bond lengths and angles of thiobases have been taken from HF/6-31G\* calculations. The C-S bond length was set to 1.6589 Å with the  $K_s$  constant of 570.0 kcal/(mol Å<sup>2</sup>). The following nonbonded parameters were assigned to the sulfur: van der Waals radius of 2.0 Å and well depth of 0.5 kcal/mol. These parameters were obtained by a fitting to extensive ab initio data available for H-bonding and stacking of thioguanine (Šponer et al., 1997). Internal cations were added into the channel either by using crystallographic data for the high-resolution parallel G-DNA structure (Phillips et al., 1997) or manually into cavities between G-quartets in all other cases. The other cations were initially placed into the most negative locations of the electrostatic potential using Coulombic potential terms with the LEAP (Case et al., 1997) module of AMBER 5.0. In simulation with a vacant channel, however, all ions were added at an equal distance from phosphate oxygen atoms spaced 3.5 Å from the phosphorus atom using the EDIT (Case et al., 1997) module of AMBER 5.0. All cations were considered as part of the solvent including those in the channel. Calculations were carried out using the Sander module of AMBER 5.0 with SHAKE on the hydrogen atoms with a tolerance of 0.0005 Å and a 2-fs time step. A 9-Å cutoff was applied to Lennard-Jones interactions. Simulations were performed using the Berendsen temperature-coupling algorithm (with a time constant of 0.2 ps). The nonbonded pair list was updated every 10 steps. Equilibration was started by 1000 steps of minimization with the positions of the nucleic acid fixed. After this initial equilibration, all subsequent simulations were performed using the particle mesh Ewald method (PME) for inclusion of long-range electrostatic interactions into calculations without truncation. The PME charge grid spacing was approximately 1.0 Å, and the charge grid was interpolated using a cubic B-spline with the direct sum tolerance of  $10^{-6}$  at the 9-Å direct space cutoff. To speed up the fast Fourier transform in the calculation of the reciprocal sum, the size of the PME charge grid was chosen to be a product of powers of 2, 3, and 5. For dynamics runs subsequent to minimizations, initial velocities were assigned from a Maxwellian distribution. Equilibration was continued by 25 ps of PME dynamics, with the position of the nucleic acid fixed. Subsequently, 1000 steps of minimization were carried out with 25 kcal/(mol Å<sup>2</sup>) restraints placed on all solute atoms, continued by 3 ps of MD simulation using the same restraint. This equilibration was followed by five rounds of 1000-step minimization with solute restraints reduced by 5 kcal/(mol Å<sup>2</sup>) in the course of each round. Then 20 ps of MD followed, with the system heated from 100 K to 300 K over 2 ps. Equilibration was continued by several nanoseconds of production simulation. It should be

noted that the simulations of thiobase-containing stems were initiated assuming the crystal geometry of unmodified  $d(\text{TG}_4\text{T})_4$ . We have thus carefully monitored the equilibration process to assure that the observed disintegration of these structures is not due to some initial energy strain. Coordinates were written to trajectory files after each picosecond. The center of mass velocity was removed during the production dynamics periodically in intervals of 10 ps.

The results were analyzed using the Carnal module of AMBER 5.0. No extra processing of the averaged structures obtained by the Carnal module was performed. Solvent distributions were monitored by binding atom positions from RMS coordinate fit frames over all DNA atoms at 1-ps intervals into 0.5-Å<sup>3</sup> grids over 1-ns portions of the trajectories (Cheatham and Kollman, 1997), with the aid of program USCF MidasPlus (Ferrin et al., 1988).

### Ab initio calculations of thioguanine-cation complexes

The structures of thioguanine- $\text{Na}^+$  complexes were optimized within the Hartree-Fock approximation utilizing the 6-311+G(d, p) basis set of atomic orbitals while the M-S6-C6 angle (M:ion) was kept frozen at a value of 135°. This constraint maintains the position of the cation with respect to guanine in a similar geometry as adopted by the cation in the G-DNA stems. However, we have further assumed an in-plane position of the cation with respect to guanine. We assume the in-plane position of a cation has no impact on the comparison with the force field but that it greatly simplifies the calculations and makes them easier to be reproduced for others. Furthermore, we calculated the dependence of the interaction energy on the interatomic S6-M<sup>+</sup> distance starting from optimized geometry and varying the S6-M<sup>+</sup> distance. The calculations were performed applying the second-order Moeller-Plesset perturbational method (MP2) with the 6-311+G(d, p) basis set and corrected for the basis set superposition error. The quantum chemical interaction energies were compared with those provided by the force field. All calculations were carried out using the Gaussian 94 set of programs (Frisch et al., 1995).

## RESULTS

### Molecular dynamics of $d(\text{GGGG})_4$ and $d(\text{III})_4$ with three cations in the channel

Let us first compare the simulations of  $d(\text{GGGG})_4$  (2.5 ns) and  $d(\text{III})_4$  (2.5 ns) with three sodium cations initially placed in the channel (Fig. 3). The  $d(\text{GGGG})_4$  quadruplex with sodium ions in the central channel is an extremely stable and rigid molecule and the only movements observed during the simulation are infrequent oscillations (bistability) of some phosphate groups. The simulated molecule is in excellent agreement with the 0.95-Å resolution crystal structure of  $d(\text{TGGGGT})_4$  (including the phosphate bistability), except for a small difference in the distribution of the  $\text{Na}^+$  cations in the channel and the occurrence of a bifurcated bonding in the inner two quartets of the simulated structure (see below). The simulated structure of  $d(\text{III})_4$  shows, on the nanosecond scale, identical structural and dynamical properties as the  $d(\text{GGGG})_4$ . The superimposed averaged structures over the last nanosecond of both the  $d(\text{GGGG})_4$  and  $d(\text{III})_4$  quadruplex simulations (Fig. 3 B) show greater deviations at the ends of the molecules than in its central part due to end effects. The heavy atom RMS



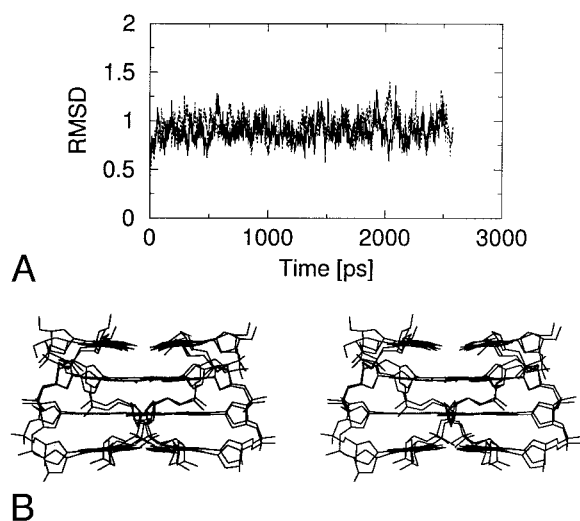


FIGURE 3 MD simulations of parallel  $d(\text{GGGG})_4$  and  $d(\text{III})_4$  quadruplexes with three  $\text{Na}^+$  cations in the channel. (A) RMS deviation (in Å) with respect to the starting structure based on 0.95-Å resolution crystal of  $d(\text{TGGGGT})_4$  (solid line, guanine quadruplex; dotted line, inosine quadruplex). (B) Stereo overlay of averaged  $d(\text{GGGG})_4$  and  $d(\text{III})_4$  molecules.

value between these average structures is 0.7 Å (superimposed after elimination of N2 amino nitrogens from guanine bases), which proves a high degree of similarity between these two structures.

As noted above, in the inner guanine quartets of the  $d(\text{GGGG})_4$  simulated structure, the bases are shifted with respect to each other such that bifurcated hydrogen bonds are formed with equidistant bond lengths ( $\sim 3.3$  Å) between the N1 nitrogen of one guanine and the N7 and O6 atoms of the adjacent guanine residue (Špačková et al., 1999). The bifurcated bonding concerns all bases in the quartet, as the quartet is symmetrical. No bifurcated bonding is observed in the outer quartets of the simulated  $d(\text{GGGG})_4$  stem. The bifurcated bonds are also absent in all inosine quartets. The distances between the N1 nitrogen of one inosine and the N7 and O6 atoms of the adjacent inosine residue is  $\sim 3.0$  and  $3.8$  Å, respectively. Again, all quartets are perfectly symmetrical.

Let us reiterate that the bifurcated H-bonding that is observed in the inner quartets in the simulation of  $d(\text{GGGG})_4$  (Špačková et al., 1999) is not in agreement with the 0.95-Å resolution crystal structure of  $d(\text{TGGGGT})_4$  (Phillips et al., 1997). The crystal shows symmetrical quartets in accordance with our simulation, but no bifurcated bonding. Due to the high quality of the crystal data we consider this experimental structure of  $d(\text{TGGGGT})_4$  to be the current reference structure for geometries of guanine quartets. It is in principle possible that the quartet geometries are affected by crystal packing forces, but we do not expect this to be the actual source of the x-ray versus MD structural difference. As explained in detail in our preceding

paper, the discrepancy between MD data and the crystal structure is likely due to a subtle force field artifact (Špačková et al., 1999), namely, due to the lack of a polarization term. This artifact cannot be repaired with the current generation of pair-additive force fields; however, it influences only the cation-solute interactions at very short distances. Therefore, it is unlikely for this imbalance to substantially affect the global geometry, stability, and dynamical properties of the quadruplex stem. The global properties are primarily determined by the electrostatic effects, which are rigorously treated by the force field and the simulation protocol. Also, it is not a primary task of our study to investigate and report the structural fine details of the simulated molecules.

It is noteworthy that the current NMR studies provide a slightly different picture of quartet geometries compared with both the x-ray and MD data. More specifically, NMR studies often show nonsymmetrical guanine quartets, i.e., quartets having two different O6-O6 distances across the channel (Strahan et al., 1998). The reason for this difference between NMR data on one side and the x-ray and MD data on the other remains to be clarified (Špačková et al., 1999). The low-resolution x-ray structure of an antiparallel guanine quadruplex (Kang et al. 1992), finally, shows considerably deformed quartet layers that are substantially different from all other NMR, x-ray, and MD structures.

The MD simulations show that the three  $\text{Na}^+$  cations within the channel are equally distributed and stay in the centers of their cavities. In contrast, the crystal structure of  $d(\text{TGGGGT})_4$  shows  $\text{Na}^+$  cations between successive guanine quartets more and more displaced in the 3' direction as the cations are close to the 3' terminus, whereas the last cation is co-planar with the outer quartet. In our opinion, this experimental cation distribution can be rationalized as a consequence of an inter-cation electrostatic repulsion with a contribution of the crystal packing effects. Note that there are seven cations lining up continuously in the crystal, positioned among eight consecutive quartets belonging to two quadruplexes. On the other hand, we have shown before (Špačková et al., 1999) that the  $\text{Na}^+$  cations in the current force field appear to be slightly oversized when placed into the quadruplex channel and it keeps them in the cavity centers for most of the time. A minor reduction of the van der Waals radius of the cation leads to a substantial temporary presence of cations in the plane of the outer guanine quartets during a simulation (Špačková et al., 1999). Let us, however, again underline that this force field adjustment is in fact not fully justified, as the inaccuracy of the force field is primarily not due to the van der Waals parameters but due to absence of the polarization term. Nevertheless, fine details of the cation distribution in the channel have probably no substantial effect on the overall quadruplex dynamics and in fact are neither within the accuracy of the technique nor the objective of our study.

A stable hydration pattern of the quadruplex stem is achieved swiftly during the first nanosecond due to the extraordinary rigidity of the solute molecule. The convergence of the hydration pattern is apparently faster compared, for example, with B-DNA duplex simulations (Štefl and Koča, 2000). The overall hydration patterns are almost identical for the guanine and inosine quadruplexes (Fig. 4). The simulated quadruplexes have clearly developed hydration sites capping the channel entrances (Špačková et al., 1999; Strahan et al., 1998). Well-organized hydration is also found around the backbone parts. The most distinguishable hydration pattern, a clear spine of hydration, is localized inside the grooves. The spine of hydration of the guanine quadruplex is more shapely and resides on the bottom of the grooves. The spine of hydration observed in the grooves of the simulated guanine quadruplex is actually quite similar to the primary hydration spine in the high-resolution crystal structure of  $d(\text{TGGGGT})_4$  (Phillips et al., 1997). The spine of hydration of the inosine quadruplex is less uniform and appears to form two layers. This is because the grooves of the inosine quadruplex are more capacious due to the absence of the amino groups. No penetration of the sodium cations into the groove's first hydration shell was evident during our simulations. The absence of cations in the grooves is in agreement with the 0.95-Å x-ray study on  $d(\text{TGGGGT})_4$  (Phillips et al., 1997). The resolution of this crystal should allow localization of close to all  $\text{Na}^+$  ions in the lattice.

### Molecular dynamics of $d(\text{GGGG})_4$ and $d(\text{IIII})_4$ with a vacant channel

To further compare properties of  $d(\text{GGGG})_4$  and  $d(\text{IIII})_4$ , we have carried out a 3-ns simulation of a vacant  $d(\text{IIII})_4$  stem and compared it with the 2.3-ns simulation of a vacant  $d(\text{GGGG})_4$  stem (Fig. 5). Both structures are apparently destabilized by the absence of the cations. The simulation of a vacant  $d(\text{GGGG})_4$  quadruplex was described in detail in our earlier study (Špačková et al., 1999). The channel was fully hydrated throughout the whole simulation, but it was not sufficient to rigidify the molecule, and large fluctuations occurred. These included mutual sliding and slippage of the strands. Nevertheless, the molecule did not disintegrate during the simulation. Large fluctuations during this simulation do not allow any meaningful structure averaging and evaluation of H-bonding patterns in the quartets.

The behavior of a vacant  $d(\text{IIII})_4$  stem is amazingly different compared with its  $d(\text{GGGG})_4$  counterpart. There is a swift and full disintegration of the all-inosine quadruplex structure within the first nanosecond. The rearrangements of the quadruplex architecture started at  $\sim 300$  ps. The strands A and D were simultaneously shifted by one base step in the 5'-end direction (see Fig. 1 for strand and base numbering). This slippage of the base-pairing interactions between maintained pairs of A-D and B-C strands leads to a structure where only two I-quartets are retained and the base pairs I4 with I16 (at the 3'end) and I5 with I9 (at the 5'end) are

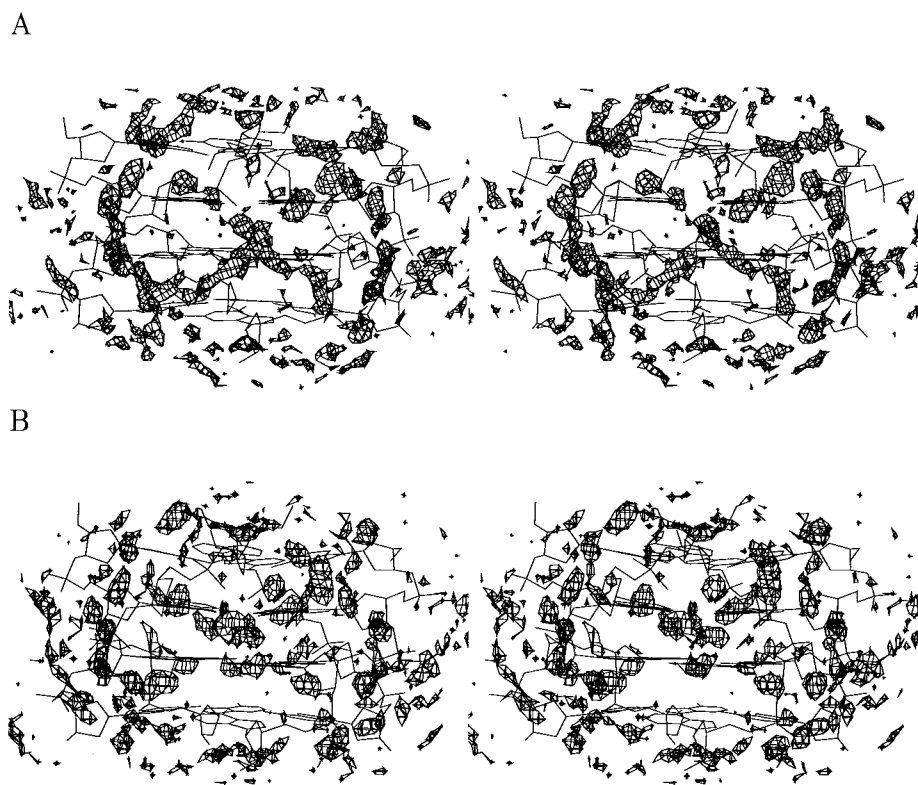


FIGURE 4 A stereo-view picture of the averaged structures and their hydration (contoured water oxygen atom density) over the last nanosecond of the parallel  $d(\text{GGGG})_4$  (A) and  $d(\text{IIII})_4$  (B) quadruplex simulations. The contours of the water oxygen density, at 1-ps intervals, into  $0.5\text{-}\text{\AA}^3$  grid elements over a  $50\text{-}\text{\AA}^3$  cubed grid, at a contour level of 15 hits per  $0.5\text{ \AA}^3$  ( $\sim 3.6$  times the bulk water density) are displayed using the density delegate from MidasPlus.

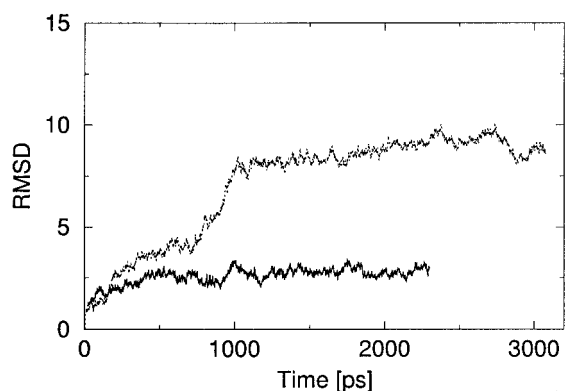


FIGURE 5 MD simulations of parallel  $d(\text{GGGG})_4$  and  $d(\text{III})_4$  quadruplexes with no cations in the channel. RMS deviation (in Å) with respect to the starting structure based on 0.95-Å resolution crystal of  $d(\text{TGGGGT})_4$  (solid line, guanine quadruplex; dotted line, inosine quadruplex).

situated at the ends of the molecule. Further rearrangements comprised a disruption of the A-D and B-C strand pairs from the 3' end. The remaining two inosine quartets have gradually been disrupted and the paired strands have been shifted away. The disintegration led at  $\sim 1$  ns to a structure already bearing no resemblance to a quadruplex. Interestingly, in this structure two strands remained H-bonded and formed a duplex, although the strands were shifted by one step. The inosine base pairs were stabilized by two  $\text{O6} \cdots \text{H1-N1}$  H-bonds. The other two strands adopted a perpendicular position to the duplex (Fig. 6).

### Molecular dynamics of $d(\text{GCGG})_4$ and $d(\text{ICII})_4$ antiparallel stems

As another attempt to highlight any differences between the respective capabilities of inosine and guanine to form quadruplex arrangements, we carried out two simulations of an antiparallel  $d(\text{ICII})_4$  stem (Fig. 1). The initial stem structure is based on the NMR structure of a  $d(\text{GCGGTTTGC GG})_2$

four-stranded hairpin duplex (Kettani et al., 1995) where the thymine loops were removed. The  $d(\text{ICII})_4$  stem is composed of two mixed inosine-cytosine quartets in its center embedded between two all-inosine quartets.

In the first simulation we have positioned two sodium cations into the outer cavities, i.e., between mixed and all-inosine quartets. It follows from our recent study that it is an optimal cation distribution for the mixed stem containing GCGC quartets (Špačková et al., submitted). When starting simulations of a mixed stem with three cations in the channel, one of them is usually swiftly eliminated on a time scale of 1 ns. The simulation of  $d(\text{ICII})_4$  was entirely stable with RMS deviations of  $\sim 1.5$  Å from the starting structure, and we did not see any conformational change during this simulation. The two Watson-Crick inosine-cytosine base pairs in the mixed quartet are hydrogen bonded through their edges, as seen in the NMR studies of mixed quadruplex stems in the presence of NaCl (Bouaziz et al., 1998; Kettani et al., 1995, 1998). We have extended this simulation up to 7 ns to verify convergence. The simulated structure was entirely stable throughout the whole simulation. Thus, inosine appears to be poised to form mixed stems equally as well as guanine. In the second simulation (3.3 ns long) no sodium cations were initially placed into the channel. However, one cation was initially placed so close to the channel entry that it moved into the channel already during the equilibration. The cation adopted the usual position between IIII and ICIC quartets and remained there during the whole simulation. The two quartets enveloping the cation were apparently stable during the simulation and the RMS deviation along the trajectory did not exceed 1.8 Å in this region. On the other hand, the outer inosine quartet at the opposite end of the molecule not stabilized by the cation reached RMS deviation of 4 Å at 0.5 ns. Its RMS value increased up to 7 Å in the course of the simulation. The quartet has been destabilized at the beginning of the simulation, and during the simulation one or more bases of this quartet have been flipped into the solvent (Fig. 7). Analo-

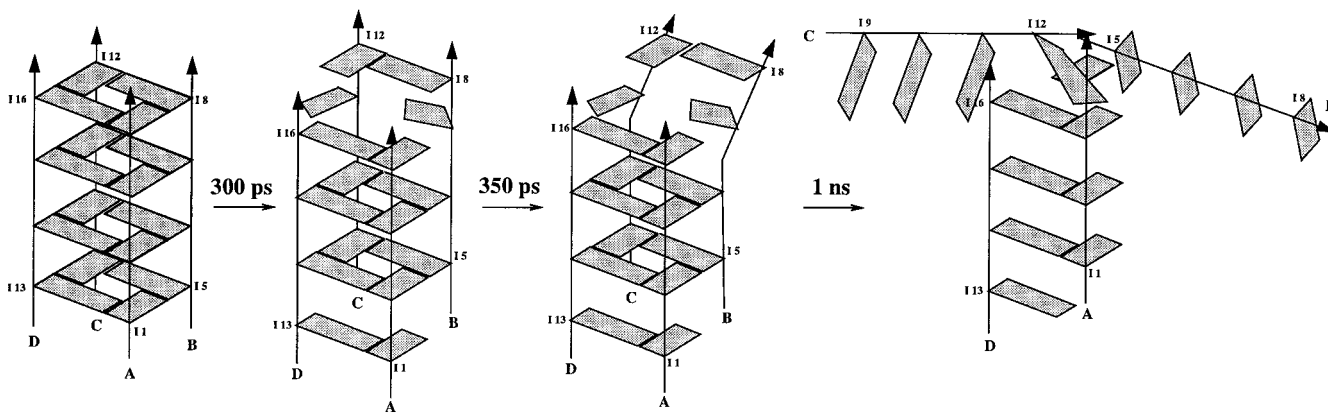


FIGURE 6 Simulation of a vacant  $d(\text{III})_4$  stem: cartoon showing the swift disintegration of the stem.

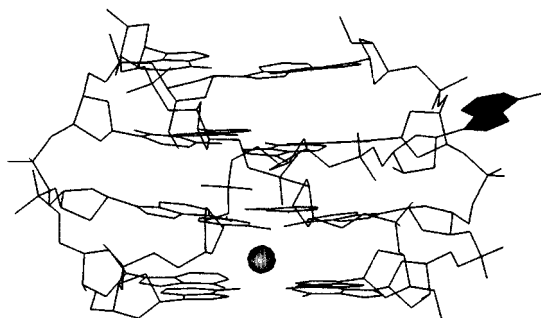


FIGURE 7 Snapshot of the  $d(\text{ICII})_4$  simulated with only one cation in the channel. Note the pronounced instability of the outer inosine quartet not stabilized by the cation.

gous simulation of  $d(\text{GCGG})_4$  with a single cation in one of the outer cavities shows almost no destabilization of the G-quartet not contacted with the cation (Špačková et al., submitted), again underlining the instability of inosine quartets in the absence of cations.

### Molecular interactions in $d(\text{GGGG})_4$ , $d(\text{IIII})_4$ , $d(\text{GCGG})_4$ , and $d(\text{ICII})_4$ stems

We have evaluated selected molecular interactions of nucleobases in the simulated structures to obtain further insight in similarities and differences between the ability of guanine and inosine to form quadruplexes. The calculations were carried out with the original AMBER force field parameters for nucleobases. The sugar-phosphate backbone

has been replaced by a hydrogen and its charge has been adjusted to keep the nucleobases neutral. All structures used in the calculations including cation positions are based on the averaged MD structures reported above. This means that all interaction energies are calculated for quartet geometries actually occurring in the quadruplexes. The results are summarized in Table 1.

The first part of Table 1 summarizes the net H-bonding energies of the quartets. The mixed quartets show the largest H-bonding contribution originating mainly in the Watson-Crick base pairing. The outer all-guanine quartet shows a considerable H-bonding stabilization with interaction energy of almost  $-45$  kcal/mol. This value is lower (in absolute value) compared with the ab initio stabilization energy of  $\sim -60$  kcal/mol reported for a fully isolated and optimized guanine quartet in gas phase (Gu et al., 1999). The difference is primarily due to adjustment of the quartet geometry induced by the cations, solvent, and other contributions that were absent in the gas phase ab initio calculations. The presently used force field well reproduces the ab initio interaction energies for H-bonded complexes of DNA bases (Hobza and Šponer, 1999). The inner all-guanine quartet enveloped by two cations and showing the bifurcated H-bonding (see above) has a considerably reduced base-base interaction in the quartet layer of  $-25$  kcal/mol. This is another indication that the H-bonding energy of the GGGG quartet depends significantly on its geometry. The all-inosine quartet shows only negligible intrinsic stabilization, and it is not surprising that this quartet without a cation swiftly disintegrates in water, as demonstrated above.

TABLE 1 Selected interaction energies (kcal/mol) in  $d(\text{GGGG})_4$ ,  $d(\text{IIII})_4$ ,  $d(\text{GCGG})_4$ , and  $d(\text{ICII})_4$  stems

System	Hydrogen bonding energy of a quartet without considering the cation		
	Coulombic term	Van der Waals term	Total interaction energy
GGGG*	-38.6	-4.9	-43.5
GGGG <sup>†</sup>	-18.0	-6.2	-24.2
IIII <sup>†</sup>	-0.7	-6.7	-7.4
GCGC <sup>‡</sup>	-63.5 (-8.4)	-3.7 (-3.6)	-67.2 (-12.0)
ICIC <sup>‡</sup>	-51.5 (-10.0)	-5.3 (-3.8)	-56.8 (-13.8)
Base stacking between two consecutive quartets without considering the cations.			
GGGG/GGGG <sup>†</sup>	+37.6	-48.8	-11.2
IIII/IIII <sup>†</sup>	+46.1	-41.4	+4.7
GCGC/GGGG	+23.9	-41.9	-18.0
ICIC/IIII	+17.7	-37.8	-20.1
GCGC/GCGC	+8.1	-36.5	-28.4
ICIC/ICIC	-0.7	-34.1	-34.8
Interaction energy between a quartet and the proximal Na <sup>+</sup> cation.			
GGGG/Na <sup>++</sup>	-110.4	+3.7	-106.7
IIII/Na <sup>++</sup>	-120.3	+4.3	-116.0
GCGC/Na <sup>+</sup>	-62.4	+3.1	-59.3
ICIC/Na <sup>+</sup>	-59.0	+3.3	-55.7

The geometries used for calculations were taken from the respective averaged MD structures having three and two cations in the channel for  $d(\text{NNNN})_4$  and  $d(\text{NCNN})_4$  stems, respectively. Cornell et al. force field and dielectric constant of 1 have been utilized.

\*Outer quartet of the all-guanine stem (data for the 3' and 5' ends are essentially identical).

<sup>†</sup>Inner quartet(s) of all-guanine (inosine) stem considered. This means a bifurcated arrangement of the all-guanine quartet (see the text).

<sup>‡</sup>The values in parentheses show the edge interaction between the two Watson-Crick base pairs (cf. Figure 1 C).



The second part of Table 1 summarizes the base stacking energies between consecutive quartets. The stacking of two all-inosine quartets is again the least stable arrangement. The mixed stems appear to have slightly better stacking than the homo-purine stems.

The last part of Table 1 shows the quartet-sodium cation interaction energies. Evidently, both GGGG and IIII quartets show a very large and attractive quartet-cation interaction, clearly dominating over the H-bonding. This explains why the two quartets behave in a similar manner when they contact a cation. The interaction between the mixed quartets and the sodium cation still shows a considerable intrinsic attraction. However, one should take into account that in solution the mixed quartets have to compete for the cations with either the solvent or the all-guanine quartet. The latter interactions are more favorable compared with the mixed quartet-cation interaction.

### Molecular dynamics of $d(\text{tGtGtGtG})_4$ , $d(\text{tltltl})_4$ , $d(\text{GtGGG})_4$ , and $d(\text{GtGGG})_4$

In the next part of the study, we investigated hypothetical all-thioguanine- and all-thiopurine-containing parallel quadruplex stems. Before the simulations, we carried out a quantum-chemical analysis of the thioguanine- $\text{Na}^+$  interaction, assuming a constrained cation-base geometry mimicking the position of the cation within the quadruplex channel (see Methods). We compared these reference data with the empirical potential values and with the data for guanine- $\text{Na}^+$  interactions (Tables 2 and 3). Tables 2 and 3 show several important features. First, the optimal distance for the thioguanine- $\text{Na}^+$  interaction is considerably larger compared with guanine, as expected. Note that also the C-S bond is considerably longer compared with the C-O one. On the other hand, the tG- $\text{Na}^+$  complex is equally as stable as the G- $\text{Na}^+$  one. Second, the force field considerably underestimates the depth of the minimum on the potential energy

**TABLE 2** Interaction energy  $\Delta E$  (in kcal/mol) between thioguanine S6 and  $\text{Na}^+$  depending on the S6- $\text{Na}^+$  distance

Distance (Å) S6- $\text{Na}^{+*}$	$\Delta E_{\text{MP2}}$ (kcal/mol) ab initio	$\Delta E_{\text{AMB}}$ (kcal/mol) empirical potential
-0.5	-12.9	+11.8
-0.4	-21.3	-6.8
-0.3	-26.2	-16.0
-0.2	-30.0	-20.5
-0.1	-31.6	-22.4
Optimal value	-32.6	-22.9
+0.1	-32.1	-22.6
+0.2	-31.4	-22.0
+0.3	-30.4	-21.1
+0.5	-28.1	-19.2

\*Distance is given with respect to the optimal value of 2.619 Å. The Na-O6-C6 angle was frozen at 135°.

**TABLE 3** Interaction energy  $\Delta E$  (in kcal/mol) between guanine O6 and  $\text{Na}^+$  depending on the O6- $\text{Na}^+$  distance to the optimal value of 2.149 Å. The Na-O6-C6 angle was frozen at 135°

Distance (Å) O6- $\text{Na}^{+*}$	$\Delta E_{\text{MP2}}$ (kcal/mol) ab initio	$\Delta E_{\text{AMB}}$ (kcal/mol) empirical potential
-0.4	-10.0	+69.5
-0.3	-21.2	+20.8
-0.2	-27.6	-2.3
-0.1	-30.9	-12.8
Optimal value	-32.2	-17.3
+0.2	-31.5	-19.0
+0.4	-28.8	-17.6
+0.6	-25.5	-15.6

\*Distance is given with respect to the optimal value of 2.149 Å. The Na-O6-C6 angle was frozen at 135°.

curve for  $\text{Na}^+$ -base interactions for both nucleobases and somewhat exaggerates the short-range repulsion between nucleobases and cations. As discussed elsewhere (Špačková et al., 1999) this inaccuracy is due to principal approximations inherent to the current generation of force fields (lack of a polarization term and atom-centered point-charge approximation) and it cannot be repaired by varying parameters within the framework of the current force field function. The force field nevertheless reproduces the relative difference between thioguanine and guanine interactions with  $\text{Na}^+$  reasonably well. In addition, for our MD simulation we primarily need the force field to provide reasonable energy gradients around the minimum energy distance, and this appears to be fulfilled.

We have carried out MD simulations of  $d(\text{tGtGtGtG})_4$  (4.5 ns) and  $d(\text{tltltl})_4$  quadruplex stems (5 ns) with initially three  $\text{Na}^+$  cations in the channel. Both simulations (Fig. 8) show pronounced deformations compared with the starting structure, in contrast to the  $d(\text{GGGG})_4$  and  $d(\text{IIII})_4$  simulations discussed above.

In the course of the simulation of  $d(\text{tGtGtGtG})_4$ , the sodium cations remained in the channel during the equilibration protocol. However, at the beginning of the simulation (at  $\sim 30$  ps) one sodium cation was expelled from the channel at the 3' end of the quadruplex. Then the strands A and B (see Fig. 1) remain to interact in the classical quadruplex manner while the strands C and D are shifted by one base step in the 5'-end direction with an apparent tilt and roll. This change occurred at  $\sim 150$  ps. The second sodium cation was expelled at  $\sim 2$  ns. However, the overall structure of the molecule described above had not changed yet. Thus the simulation resulted in a structure that was not fully disintegrated on the nanosecond scale, but was considerably different from the native  $d(\text{GGGG})_4$  stem and included one cation buried inside the collapsing stem (Fig. 8 B).

Even larger changes were noticed in the course of the  $d(\text{tltltl})_4$  simulation. One sodium cation was expelled from

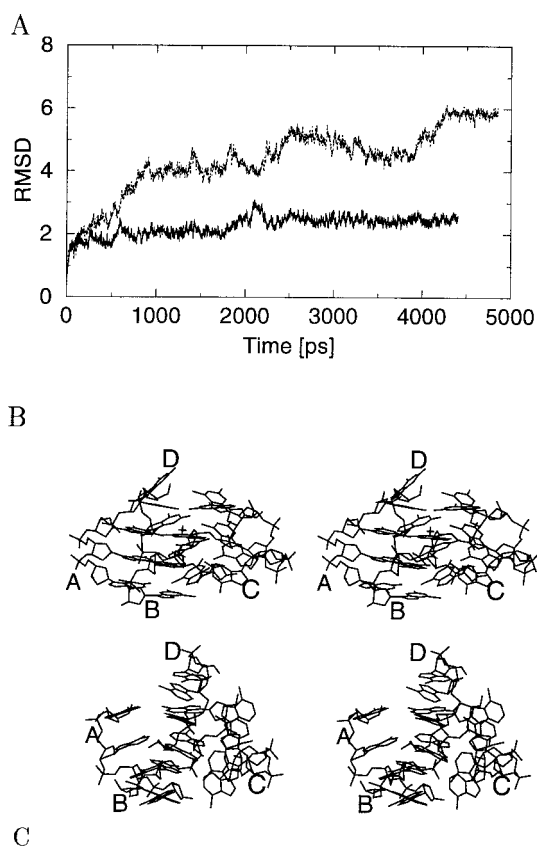


FIGURE 8 MD simulations of parallel  $d(tGtGtGtG)_4$  and  $d(tlftlftl)_4$  quadruplexes with initially three cations in the channel. (A) RMS deviation (in Å) with respect to the starting structure based on 0.95-Å resolution crystal of  $d(TGGGGT)_4$  (solid line, thioguanine quadruplex; dotted line, thioinosine quadruplex). (B) Stereo picture of the  $d(tGtGtGtG)_4$  simulated structure averaged over the last nanosecond, the position of the last cation remaining inside is indicated by +. (C) Stereo picture of the  $d(tlftlftl)_4$  simulated structure averaged over the last nanosecond. Strands are indicated as in Fig. 1.

the channel already during the equilibration. The second sodium cation left the channel at  $\sim 300$  ps during the production simulation. The last sodium ion was eliminated from the structure at  $\sim 2.5$  ns. The starting quadruplex stem structure completely collapsed during the simulation and showed no similarity to the original quadruplex (Fig. 8 C).

We have carried out two additional simulations with one and four guanines in the original  $d(GGGG)_4$  stem replaced by thioguanines. In the first simulation (3 ns), we have inserted one thioguanine into the second quartet of the stem. The simulation was quite stable, although a closer inspection reveals that the stem geometry locally oscillates between two substates with a periodicity of 50–200 ps. The first conformation is the usual stem, although the sodium cations are slightly shifted away from the thioguanine residue. The second conformation is characterized by one cation positioned in the plane of the first quartet. The thioguanine placed in the second quartet is slightly buckled toward the first quartet whereas the central cation is slightly shifted toward the second quartet. In the subsequent simulation (3.1 ns) we replaced the whole second quartet by a thioguanine quartet. This resulted in a marked stress in the structure (Fig. 9). At the beginning of the simulation all thioguanines buckle toward the center of the stem, shifting the second and third cation into planes of the third and fourth quartet, respectively. The third cation even moves outside the channel. The structure essentially repairs at 200 ps, but shortly after the whole thioguanine quartet buckles in the opposite direction, pushing the proximal cation into the plane of the terminal quartet. This geometry persisted until 1.0 ns, when the cation moved outside the channel and the outer quartet is markedly destabilized. The structure reaches the maximum RMS deviation at  $\sim 1.7$  ns, when the cation is returning close to the channel entry; however, it does not enter the channel. At the very end of the simulation the cation again leaves the stem and the outer quartet is destabilized.

Finally, we have carried out an additional 3-ns simulation of a parallel-stranded all-thioguanine quadruplex  $d(tGtGtGtG)_4$  in the presence of  $Li^+$ , again initially with three cations in the channel. The first cation was eliminated from the quadruplex channel at  $\sim 0.5$  ns, and a second one at  $\sim 2.5$  ns. The quadruplex stem shows extensive fluctuations and mutual shifts of the strands already in the early stages of the simulations. At the end of the simulation, the RMS deviation of the stem with respect to the starting geometry reaches as much as 4 Å and the structure is largely deformed. This simulation convincingly predicts that  $d(tGtGtGtG)_4$

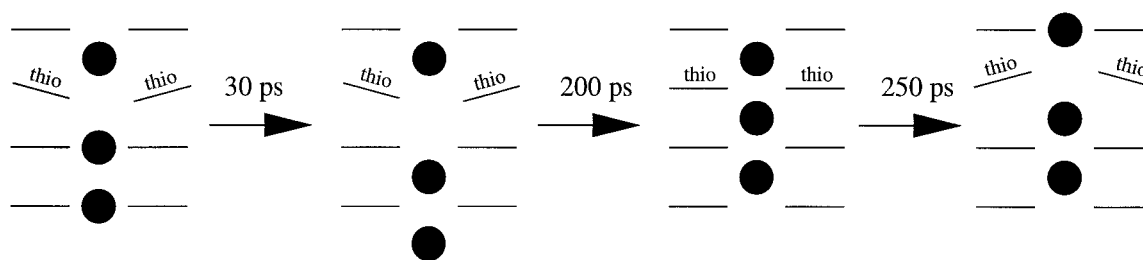


FIGURE 9 MD simulations of parallel  $d(GtGGG)_4$  quadruplex with three  $Na^+$  cations initially placed into the channel: sketch of thioguanine buckling and sodium cations shifting observed during the simulation.

$\text{GtG}_4$  quadruplex is unstable even in presence of the smallest  $\text{Li}^+$  cation.

## DISCUSSION

We have carried out a set of explicit-solvent, nanosecond-scale, unrestrained simulations of four-stranded G-DNA stems, containing the modified bases 6-oxopurine, 6-thioguanine, and 6-thiopurine and compared the results with those obtained for all-guanine quadruplexes. The simulations represent an extension of our preceding studies of four-stranded DNA assemblies (Špačková et al., 1998, 1999, submitted).

The simulations show that inosine is capable of forming cation-stabilized all-inosine as well as mixed inosine-cytosine quadruplex stems with identical (on the nanosecond scale) properties as the native structures with guanine. This mainly means a presence of cation-stabilized inosine quartets and exceptional rigidity of the stem. The loss of all amino groups implies a loss of four hydrogen bonds per quartet, although no apparent destabilization is seen. This clearly indicates that the stems are primarily stabilized by the quartet-cation interactions, which are very similar for inosine and guanosine due to close similarity in their electronic structures (Šponer et al., 1996).

In contrast, simulation of a hypothetical structure of a parallel all-inosine stem with a vacant channel revealed a striking difference between guanine's and inosine's ability to form quadruplexes, which is not apparent when simulating just the final cation-stabilized stems. When removing all cations from the channel, both  $\text{d}(\text{GGGG})_4$  and  $\text{d}(\text{IIII})_4$  stems are destabilized; thus the vacant stem structure is an unstable stage for both molecules. However, the vacant guanine-containing stem does not disintegrate on the nanosecond scale, despite its fluctuations. This in fact gives the molecule enough time to intercept a cation from solvent and to achieve stabilization. On the other hand a vacant  $\text{d}(\text{IIII})_4$  stem disintegrates immediately and completely and has no time to catch any cation. In other words, on a longer time scale, we expect that the initially vacant  $\text{d}(\text{GGGG})_4$  stem would be converted into a native cation-stabilized stem whereas the initially vacant  $\text{d}(\text{IIII})_4$  disintegrates. Thus these simulations give us an unprecedented insight into possible differences in the process of formation of guanine and inosine quadruplexes. Both molecules behave in the same way when fully soaked by the monovalent cations, as the cation-quartet contribution is the dominating stabilization term. However, when the molecules have to rely on the H-bond stabilization due to the lack of cations they may behave very differently. Formation of a cation-stabilized quadruplex is an exceptionally slow process with complex kinetics and it certainly involves long-living intermediates very different from the final structure. One can hardly assume that four strands and three cations are simultaneously coming together to form the stem. It is reasonable

to assume that some of the intermediate structures are stabilized by conventional base-base H-bonds rather than by cation-base interactions (Han et al., 1999a; Hardin et al., 1997), and for such structures the guanine-inosine difference can be very significant. Thus we speculate that formation of guanine and inosine quadruplexes might proceed via a different sequence of intermediates. We can also imagine a situation when a formation of an inosine quadruplex is kinetically blocked or hindered due to instability of some key intermediates despite that the final quadruplex itself would be stable. The vacant stem is an example of such a structure. If  $\text{dG}_4$  reaches this structure, then formation of the quadruplex is likely to proceed smoothly. However, this would not be the case for  $\text{dI}_4$ . Of course it does not mean that we suggest vacant stems are the actual major intermediates in a quadruplex formation. Nevertheless, formation of a parallel all-guanine stem could in principle involve this state, as a result of either stepwise strand addition or duplex dimerization (cf. Fig. 10 in Hardin et al., 1997). However, there seems to be no reasonable way to form an all-inosine stem through this process, and for the all-inosine stem, active cation coordination in earlier stages of the quadruplex formation appears to be vital. Work is in progress in our laboratories to further investigate alternative folding patterns and possible intermediates for quadruplex formation.

Several recent experimental studies investigated an exchange of cations between the central ion channel of the quadruplex stem and bulk solvent. Hud and coworkers (1999) applied  $^1\text{H}$  and  $^{15}\text{N}$  heteronuclear NMR spectroscopy on the bimolecular quadruplex  $[\text{d}(\text{G}_4\text{T}_4\text{G}_4)]_2$  in the presence of ammonium ions. They have shown that a full exchange of ammonium ions occurs on a millisecond time scale with the average cation residence time being  $\sim 250$  ms. Earlier work (Deng and Braulin, 1996) deals with the same type of quadruplex in the presence of sodium ions. This study suggests a lifetime of a bound  $\text{Na}^+$  to be  $\sim 250$   $\mu\text{s}$ . These experiments, unfortunately, cannot be directly compared with the present simulations carried out on the nanosecond time scale only.

Simulations of quadruplexes with thioguanine and thioinosine convincingly show that  $\text{dtG}_4$  and  $\text{dtI}_4$  do not have any ability to form cation-stabilized quadruplexes. Although the thiogroup has a very favorable interaction with  $\text{Na}^+$ , this group is too bulky and its presence leads to expulsion of the cations from the channel and a collapse of the quadruplex structure on the nanosecond scale. When only one thioguanine is incorporated into the stem, the structure remains stable, although local fluctuations around the thioguanine are seen. This behavior is in agreement with experiments suggesting that one thioguanine can be incorporated although the structure becomes less stable (Gee et al., 1995; Marathias et al., 1999; Olivas and Maher, 1995; Rao et al., 1995). When a whole thioguanine quartet is incorporated the structure appears to be quite disturbed,

although it does not disintegrate on the nanosecond time scale.

Modern nanosecond-scale, unrestrained, explicit-solvent MD simulations carried out with the aid of an accurate method for the treatment of electrostatic interactions (PME) represent a robust technique to study the structure and dynamics of oligonucleotides. Nevertheless, even the accuracy of such a state-of-the-art computational tool has limitations caused by the approximations inherent to the force field (cf. the *ab initio* and force field data in Tables 2 and 3) and time scale of the simulations. We do not intend to discuss these limitations in this contribution, as the reader can find detailed discussions for quadruplexes in our preceding reports (Špačková et al., 1998, 1999, submitted). Let us nevertheless comment on the approximation we believe is the most critical one for evaluation of the outcome of the studies presented here, namely, the limited accuracy of the description of direct cation-solute interactions. The pair-additive force field has a limited ability to treat interactions of metal cations, even for monovalent alkaline species. Due to the neglect of polarization contributions, the strength of interactions involving cations is in general underestimated by the force field. At the same time, the Lennard-Jones van der Waals term is too steep in its repulsive region; i.e., for short cation-ligand distances the short-range repulsion is exaggerated by the force field. As demonstrated elsewhere, with standard AMBER parameters the  $\text{Na}^+$  cation in fact appears to be a little oversized when placed into a guanine quadruplex stem (Špačková et al., 1999). Because we concluded in the present study that the thio base destabilizes quadruplexes primarily through steric repulsion one can argue that the overestimated short-range repulsion is an issue to be concerned about. This is one of the reasons why the current simulations were performed using  $\text{Na}^+$  AMBER parameters rather than  $\text{K}^+$  although the relevant experiments were done in a  $\text{K}^+$  environment. When using the AMBER model of  $\text{Na}^+$  in the simulations, we in fact carry out the simulation with a particle with short-range repulsion effects somewhere in-between the short-range repulsion that would be exerted by real  $\text{Na}^+$  on the one hand and real  $\text{K}^+$  on the other (though obviously being still closer to a real sodium). Thus such simulations represent a lower estimate of the actual steric effects that would accompany a placement of a genuine  $\text{K}^+$  into the thioguanine quadruplex stem. Genuine  $\text{K}^+$  would exert even stronger destabilization effects on the thio-G-containing quadruplex than seen in our simulations. The simulations are in our opinion entirely relevant with respect to the available experimental data in the presence of KCl. Nevertheless, based on the degree and speed of the destruction of the  $\text{d}(\text{tG}_4)_4$  stem we predict that such a quadruplex cannot be stabilized by any cation, as confirmed explicitly by the simulation considering  $\text{Li}^+$  cations in the channel.

## CONCLUSIONS

The ability of G-DNA to incorporate the nonstandard purine bases 6-oxopurine (inosine, I), 6-thioguanine (tG), and 6-thiopurine (tI) has been investigated using large-scale MD simulations with explicit inclusion of water and counterions. The simulations were carried out using the AMBER program package, utilizing the Cornell et al. force field, and long-range electrostatic interactions were treated using the PME technique. The length of the simulations presented reaches a total of 26 ns.

Our simulations demonstrate that inosine is well positioned to be incorporated into G-DNA stems. Even the all-inosine quadruplex stem  $\text{d}(\text{III})_4$  shows identical structural and dynamical properties as  $\text{d}(\text{GGGG})_4$  on the nanosecond scale despite the lack of four H-bonds in all inosine quartets as compared with all-guanine quartets. The reason is that both  $\text{d}(\text{GGGG})_4$  and  $\text{d}(\text{III})_4$  quadruplexes are primarily stabilized by interactions between the monovalent cations residing in the channel of the stem and the exocyclic carbonyl groups of the nucleobase quartets. This is explained by the similarity in the electronic structures of guanine and inosine.

Notwithstanding, simulations carried out lacking monovalent cations in the channel identify dramatic differences in the behavior of  $\text{d}(\text{GGGG})_4$  and  $\text{d}(\text{III})_4$ . A vacant  $\text{d}(\text{GGGG})_4$  stem shows large fluctuations but does not disintegrate. Our recent study on mixed G-DNA stems (Špačková et al., submitted) indicates that a vacant G-DNA stem is able to intercept and attract a cation from the bulk solvent on a time scale of  $\sim 10$  ns to achieve its basic stabilization. However, vacant  $\text{d}(\text{III})_4$  is irreversibly disrupted within the first nanosecond of simulation without having much of a chance to incorporate a cation. The absence of channel cations leads to a full manifestation of the lack of H-bonds involving the missing N2 amino group. We hypothesize that this difference between guanine and inosine quartets may affect, for example, the process of the folding of the respective quadruplexes. More specifically, the actual process of a formation of  $\text{d}(\text{III})_4$  could involve different intermediates compared with a formation  $\text{d}(\text{GGGG})_4$ . One can also imagine a situation when a formation of the inosine-containing quadruplex is hindered due to the instability of some key H-bonded intermediates that would be stable in presence of the N2 amino group, similar to what was observed in a simulation of the vacant  $\text{d}(\text{III})_4$  molecule. We are, however, aware of the fact that relevant experimental data do not exist at this time to assess the relevance of our suggestions, rendering these to some extent speculative. Nevertheless, it is our opinion that the contemporary MD technique is a robust and solid methodology capable of making useful predictions even in the absence of relevant experimental data, and in our view it is useful to highlight the differences between guanine- and inosine-quartet-containing molecules.



Experiments clearly demonstrate that thioguanine inhibits the formation of G-DNA. Our simulations provide the first atomic insight into this process. The G-DNA stem is able to incorporate a single thioguanine base although it already leads to minor local perturbations of the structure indicating some destabilization. Incorporation of a whole thioguanine quartet is associated with a large perturbation of the G-DNA stem already on the nanosecond time scale and this molecule appears to be unstable on a long time scale. This sharply contrasts the exceptional stability characteristic for the native G-DNA stem. When all guanines are replaced by thioguanines the stem immediately collapses. Incorporation of thiopurine leads to an even faster disintegration of the quadruplex.

The main reason for the destabilization of G-DNA by thioguanine and thiopurine is the size of the thiogroup. This leads to insurmountable steric conflicts in the quadruplex channel and expels the cations out of the channel of the quadruplex stem. The electrostatic interaction between monovalent alkaline cations and the thiogroup per se is as favorable as for the carbonyl group.

The results of our study show agreement with all available experimental data and summarily demonstrate the usefulness of a large-scale MD simulation technique in the analysis of unusual DNA assemblies and their molecular interactions.

This study was supported by grant A4040903 from the Agency of the Academy of Sciences of the Czech Republic, by grant VS96095 from the Ministry of Education of the Czech Republic, and by grant 203/00/0633 from the Agency of the Czech Republic. I.B. was supported by a Liebig fellowship from the Fonds der Chemischen Industrie, Germany. All calculations were carried out in Supercomputer Center Brno.

## REFERENCES

- Aboul-ela, F., A. I. Murchie, D. G. Norman, and D. M. Lilley. 1994. Solution structure of a parallel-stranded tetraplex formed by d(TG<sub>4</sub>T) in the presence of sodium ions by nuclear magnetic resonance spectroscopy. *J. Mol. Biol.* 243:458–471.
- Akman, S. A., R. G. Lingeman, J. H. Doroshov, and S. S. Smith. 1991. Quadruplex DNA formation in a region of the tRNA gene supF associated with hydrogen peroxide mediated mutations. *Biochemistry*. 30: 8648–8653.
- Arnott, S., R. Chandrasekaran, and C. M. Marttila. 1974. Structures for polyinosinic acid and polyguanylic acid. *Biochem. J.* 141:537–543.
- Bouaziz, S., A. Kettani, and D. J. Patel. 1998. A K cation-induced conformational switch within a loop spanning segment of a DNA quadruplex containing G-G-G-C repeats. *J. Mol. Biol.* 282:637–652.
- Case, D. A., D. A. Pearlman, J. W. Caldwell, T. E. Cheatham III, W. S. Ross, C. L. Simmerling, T. A. Darden, K. M. Merz, R. V. Stanton, A. L. Cheng, J. J. Vincent, M. Crowley, D. M. Ferguson, R. J. Radmer, G. L. Seibel, U. C. Singh, P. K. Weiner, and P. A. Kollman. 1997. AMBER. University of California, San Francisco.
- Cech, T. R. 1988. G-strings at chromosome ends. *Nature*. 332:777–778.
- Cheatham, T. E., III, P. Cieplak, and P. A. Kollman. 1999. A modified version of the Cornell et al. force field with improved sugar pucker phases and helical repeat. *J. Biomol. Struct. Dyn.* 16:845–862.
- Cheatham, T. E., III, and P. A. Kollman. 1997. Molecular dynamics simulations highlight the structural differences among DNA:DNA, RNA:RNA, and DNA:RNA hybrid duplexes. *J. Am. Chem. Soc.* 119: 4805–4825.
- Cheatham, T. E., III, J. L. Miller, T. Fox, T. A. Darden, and P. A. Kollman. 1995. Molecular dynamics simulations on solvated biomolecular systems: the particle mesh Ewald method leads to stable trajectories of DNA, RNA, and proteins. *J. Am. Chem. Soc.* 117:4193–4194.
- Cheatham, T. E., III, J. Srinivasan, D. A. Case, and P. A. Kollman. 1998. Molecular dynamics and continuum solvent studies of the stability of polyG-polyC and polyA-polyT DNA duplexes in solution. *J. Biomol. Struct. Dyn.* 16:265–280.
- Cornell, W. D., P. Cieplak, C. I. Bayly, I. R. Gould, K. M. Merz, Jr., D. M. Ferguson, D. C. Spellmeyer, T. Fox, J. W. Caldwell, and P. A. Kollman. 1995. A second generation force field for the simulation of proteins, nucleic acids, and organic molecules. *J. Am. Chem. Soc.* 117: 5179–5197.
- Deng, H., and W. H. Brulin. 1996. Kinetics of sodium ion binding to DNA quadruplexes. *J. Mol. Biol.* 255:476–483.
- Feig, M., and B. M. Pettitt. 1998. Structural equilibrium of DNA represented with different force fields. *Biophys. J.* 75:134–149.
- Feig, M., and B. M. Pettitt. 1999. Sodium and chlorine ions as part of the DNA solvation shell. *Biophys. J.* 77:1769–1781.
- Ferrin, T. E., C. C. Huang, L. E. Jarvis, and R. Langridge. 1988. The MIDAS display system. *J. Mol. Graph.* 6:13–27.
- Frisch, M. J., G. W. Trucks, H. B. Schlegel, P. M. W. Gill, B. G. Johnson, M. A. Robb, J. R. Cheeseman, T. Keith, G. A. Petersson, J. A. Montgomery, K. Raghavachari, M. A. Al-Laham, W. G. Zakrzewski, J. V. Ortiz, J. B. Foresman, Y. C. Peng, P. Y. Ayala, W. Chen, M. W. Wong, L. J. Andres, E. S. Replogle, R. Gomperts, R. L. Martin, D. J. Fox, J. S. Binkley, D. J. Defrees, J. Baker, J. J. P. Stewart, M. Head-Gordon, C. Gonzalez, J. A. Pople. 1995. Gaussian 94. Gaussian Inc., Pittsburgh.
- Folloppe, N., A. D. MacKerrel, Jr. 2000. All-atom empirical force field for nucleic acids. I. Parameter optimization based on small molecule and condensed phase macromolecular target data. *J. Comput. Chem.* 21: 86–104.
- Gee, J. E., G. Revankar, R., S. Rao, T., and M. E. Hogan. 1995. Triplex formation at the rat *neu* gene utilizing imidazole and 2'-deoxy-6-thioguanosine base substitutions. *Biochemistry*. 34:2042–2048.
- Gu, J., J. Leszczynski, and M. Bansal. 1999. A new insight into the structure and stability of Hoogsteen hydrogen-bonded G-tetrads: an ab initio SCF study. *Chem. Phys. Lett.* 311:209–214.
- Han, H., C. L. Cliff, and L. H. Hurley. 1999a. Accelerated assembly of G-quadruplex structures by a small molecule. *Biochemistry*. 38: 6981–6986.
- Han, F. X., R. T. Wheelhouse, and L. H. Hurley. 1999b. Interactions of TMPyP4 and TMPyP2 with quadruplex DNA: structural basis for the differential effects on telomerase inhibition. *J. Am. Chem. Soc.* 121: 3561–3570.
- Hardin, C. C., M. J. Corregan, D. V. Lieberman, and B. A. Brown II. 1997. Allosteric interactions between DNA strands and monovalent cations in DNA quadruplex assembly: thermodynamic evidence for three linked association pathways. *Biochemistry*. 36:15428–15450.
- Hardin, C. C., and W. S. Ross. 1994. Ion induced stabilization of G-DNA quadruplexes: free energy perturbation studies. *J. Am. Chem. Soc.* 116: 6080–6194.
- Henderson, E., C. C. Hardin, S. K. Walk, I. Tinoco, Jr., and E. H. Blackburn. 1987. Telomeric DNA oligonucleotides form novel intramolecular structures containing guanine-guanine base pairs. *Cell*. 51: 899–908.
- Hobza, P., and J. Šponer. 1999. Structure, energetics, and dynamics of the nucleic acid base pairs: nonempirical ab initio calculations. *Chem. Rev.* 99:3247–3276.
- Hud, N. V., P. Schultze, V. Sklenář, and J. Feigon. 1999. Binding sites and dynamics of ammonium ions in a telomere repeat DNA quadruplex. *J. Mol. Biol.* 285:233–243.
- Jorgensen, W. L., J. Chandrasekhar, J. D. Madura, R. W. Impey, and M. L. Klein. 1983. Comparison of simple potential functions for simulating liquid water. *J. Chem. Phys.* 79:926–935.

- Kang, C., X. Zhang, R. Ratliff, R. Moyzis, and A. Rich. 1992. Crystal structure of four-stranded *Oxytricha* telomeric DNA. *Nature*. 356: 126–131.
- Kettani, A., S. Bouaziz, A. Gorin, H. Zhao, R. A. Jones, and D. J. Patel. 1998. Solution structure of a Na cation stabilized DNA quadruplex containing GGGG and GCGC tetrads formed by G-G-G-C repeats observed in adeno-associated viral DNA. *J. Mol. Biol.* 282:619–636.
- Kettani, A., R. A. Kumar, and D. J. Patel. 1995. Solution structure of a DNA quadruplex containing the fragile X syndrome triplet repeat. *J. Mol. Biol.* 254:638–656.
- Klobutcher, L. A., M. T. Swanton, P. Donini, and D. M. Prescott. 1981. All gene-sized DNA molecules in four species of hypotrichs have the same terminal sequence and an unusual 3' terminus. *Proc. Natl. Acad. Sci. U.S.A.* 78:3015–3019.
- Konerding, D. E., T. E. Cheatham III, P. A. Kollman, and T. L. James. 1999. Restrainted molecular dynamics of solvated duplex DNA using the particle mesh Ewald method. *J. Biomol. NMR*. 13:119–131.
- Langley, D. R. 1998. Molecular dynamic simulations of environment and sequence dependent DNA conformations: the development of the BMS nucleic acid force field and comparison with experimental results. *J. Biomol. Struct. Dyn.* 16:487–509.
- Laughlan, G., A. I. H. Murchie, D. G. Norman, M. H. Moore, P. C. E. Moody, D. M. J. Lilley, and B. Luisi. 1994. The high-resolution crystal structure of a parallel-stranded guanine tetraplex. *Science*. 265:520–524.
- Lipps, H. J., W. Gruißem, and D. M. Prescott. 1982. Higher order DNA structure in macronuclear chromatin of the hypotrichous ciliate *Oxytricha nova*. *Proc. Natl. Acad. Sci. U.S.A.* 79:2495–2499.
- Louise-May, S., P. Auffinger, and E. Westhof. 1996. Calculations of nucleic acid conformations. *Curr. Opin. Struct. Biol.* 6:289–298.
- Marathias, V. M., M. J. Sawicki, and P. H. Bolton. 1999. 6-Thioguanine alters the structure and stability of duplex DNA and inhibits quadruplex DNA formation. *Nucleic Acids Res.* 27:2860–2867.
- Mergny, J. L., P. Mailliet, F. Lavelle, J. F. Riou, A. Laoui, and C. Helene. 1999. The development of telomerase inhibitors: the G-quartet approach. *Anticancer Drug Res.* 14:327–339.
- Mohanty, D., and M. Bansal. 1994. Conformational polymorphism in telomeric structures: loop orientation and interloop pairing in  $d(G_4T_nG_4)$ . *Biopolymers*. 34:1187–1211.
- Mohanty, D., and M. Bansal. 1995. Chain folding and A:T pairing in human telomeric DNA: a model-building and molecular dynamics study. *Biophys. J.* 69:1046–1067.
- Moyzis, R. K., J. M. Buckingham, L. S. Cram, M. Dani, L. L. Deaven, M. D. Jones, J. Meyne, R. L. Ratliff, and J.-R. Wu. 1988. A highly conserved repetitive DNA sequence, (TTAGGG)<sub>n</sub>, present at the telomeres of human chromosomes. *Proc. Natl. Acad. Sci. U.S.A.* 85: 6622–6626.
- Murchie, A. I., and D. M. Lilley. 1992. Retinoblastoma susceptibility genes contain 5' sequences with a high propensity to form guanine-tetrad structures. *Nucleic Acids Res.* 20:49–53.
- Oka, Y., and C. A. Thomas, Jr. 1987. The cohering telomeres of *Oxytricha*. *Nucleic Acids Res.* 15:8877–8898.
- Olivas, W. M., and L. J. Maher. 1995. Overcoming potassium-mediated triplex inhibition. *Nucleic Acids Res.* 23:1936–1941.
- Pearlman, D. A., D. A. Case, J. W. Caldwell, W. S. Ross, T. E. Cheatham III, S. DeBolt, D. M. Ferguson, G. L. Seibel, and P. A. Kollman. 1995. AMBER, a package of computer programs for applying molecular mechanics, normal mode analysis, molecular dynamics and free energy calculations to simulate the structural and energetic properties of molecules. *Comp. Phys. Commun.* 91:1–41.
- Phillips, K., Z. Dauter, A. I. H. Murchie, D. M. J. Lilley, and B. Luisi. 1997. The crystal structure of a parallel-stranded guanine tetraplex at 0.95 angstrom resolution. *J. Mol. Biol.* 273:171–182.
- Rao, T. S., R. H. Durland, D. M. Seth, M. A. Myrick, V. Bodepudi, and G. R. Revankar. 1995. Incorporation of 2'-deoxy-6-thioguanosine into G-rich oligodeoxyribonucleotides inhibits G-tetrad formation and facilitates triplex formation. *Biochemistry*. 34:765–772.
- Read, M. A., A. A. Wood, J. R. Harrison, S. M. Gowan, L. R. Kelland, H. S. Dosanji, and S. Neidle. 1999. Molecular modeling studies on G-quadruplex complexes of telomerase inhibitors: structure-activity relationships. *J. Med. Chem.* 42:4538–4546.
- Schultze, P., N. V. Hud, F. W. Smith, and J. Feigon. 1999. The effect of sodium, potassium and ammonium ions on the conformation of the dimeric quadruplex formed by the *Oxytricha nova* telomere repeat oligonucleotide  $d(G(4)T(4)G(4))$ . *Nucleic Acids Res.* 27:3018–3028.
- Sen, D., and W. Gilbert. 1988. Formation of parallel four-stranded complexes by guanine-rich motifs in DNA and its implications for meiosis. *Nature*. 334:364–366.
- Shields, G. C., C. A. Laughton, and M. Orozco. 1997. Molecular dynamics simulations of the  $d(T.A.T)$  triple helix. *J. Am. Chem. Soc.* 119: 7463–7469.
- Smith, F. W., and J. Feigon. 1992. Quadruplex structure of telomeric DNA oligonucleotides. *Nature*. 356:164–168.
- Smith, F. W., P. Schultze, and J. Feigon. 1995. Solution structures of unimolecular quadruplexes formed by oligonucleotides containing *Oxytricha* telomere repeats. *Structure*. 3:997–1008.
- Špačková, N., I. Berger, M. Egli, and J. Šponer. 1998. Molecular dynamics of hemiprotonated intercalated four-stranded i-DNA: Stable trajectories on a nanosecond scale. *J. Am. Chem. Soc.* 120:6147–6151.
- Špačková, N., I. Berger, and J. Šponer. 1999. Nanosecond molecular dynamics simulations of parallel and antiparallel guanine quadruplex DNA molecules. *J. Am. Chem. Soc.* 121:5519–5534.
- Šponer, J., J. V. Burda, J. Leszczynski, and P. Hobza. 1999. Interactions of hydrated IIa and IIb group metal cations with thioguanine-cytosine DNA base pair: ab initio and density functional theory investigation of polarization effects, differences among cations, and flexibility of the cation hydration shell. *J. Biomol. Struct. Dyn.* 17:61–77.
- Šponer, J., J. Leszczynski, and P. Hobza. 1996. Structures and energies of hydrogen-bonded DNA base pairs: a nonempirical study with inclusion of electron correlation. *J. Phys. Chem.* 100:1965–1974.
- Šponer, J., J. Leszczynski, and P. Hobza. 1997. Thioguanine and thiouracils: hydrogen-bonding and stacking properties. *J. Phys. Chem.* 101:9489–9495.
- Sprou, D., M. A. Young, and D. L. Beveridge. 1999. Molecular dynamics studies of axis bending in  $d(G_5-(GA_4T_4C)_2-C_5)$  and  $d(G_5-(GT_4A_4C)_2-C_5)$ : effects of sequence polarity on DNA curvature. *J. Mol. Biol.* 285:1623–1632.
- Štefl, R., and J. Koča. 2000. Unrestrained molecular dynamics simulations of  $[d(AT)_2]$  duplex in aqueous solution: hydration and binding of sodium ions in the minor groove. *J. Am. Chem. Soc.* 123:5025–5033.
- Strahan, G. D., M. A. Keniry, and R. H. Shafer. 1998. NMR structure refinement and dynamics of the  $K^+-[d(G_3T_4G_3)]_2$  quadruplex via particle mesh Ewald molecular dynamics simulations. *Biophys. J.* 75: 968–981.
- Strahan, G. D., R. H. Shafer, and M. A. Keniry. 1994. Structural properties of the  $[d(G_3T_4G_3)]_2$  quadruplex: evidence for sequential syn-syn deoxyguanosines. *Nucleic Acids Res.* 22:5447–5455.
- Sundquist, W. I. 1993. Conducting the G-quartet. *Curr. Opin. Struct. Biol.* 3:893–895.
- Sundquist, W. I., and S. Heaphy. 1993. Evidence for interstrand quadruplex formation in the dimerization of human immunodeficiency virus 1 genomic RNA. *Proc. Natl. Acad. Sci. U.S.A.* 90:3393–3397.
- Sundquist, W. I., and A. Klug. 1989. Telomeric DNA dimerizes by formation of guanine tetrads between hairpin loops. *Nature*. 342: 825–829.
- Trantírek, L., R. Štefl, M. Vorlíčková, J. Koča, V. Sklenář, and J. Kypr. 2000. An A-type double helix of DNA having B-type puckering of the deoxyribose rings. *J. Mol. Biol.* 297:907–922.
- Weerasinghe, S., P. E. Smith, and B. M. Pettitt. 1995. Structure and stability of a model pyrimidine-purine-purine DNA triple helix with a GC.T mismatch by simulation. *Biochemistry*. 34:16269–16278.
- Williamson, J. R., M. K. Raghuraman, and T. R. Cech. 1989. Monovalent cation-induced structure of telomeric DNA: the G-quartet model. *Cell*. 59:871–880.
- Young, M. A., and D. L. Beveridge. 1998. Molecular dynamics simulations of an oligonucleotide duplex with adenine tracts phased by a full helix turn. *J. Mol. Biol.* 281:675–687.
- Young, M. A., B. Jayaram, and D. L. Beveridge. 1997. Intrusion of counterions into the spine of hydration in the minor groove of B-DNA: fractional occupancy of electronegative pockets. *J. Am. Chem. Soc.* 119:59–69.